Theoretical and (e,2e) Experimental Investigation into the Complete Valence Electronic Structure of [1.1.1]Propellane

W. Adcock[†] M. J. Brunger,*[,‡] C. I. Clark,[†] I. E. McCarthy,[‡] M. T. Michalewicz,[§] W. von Niessen,[||] E. Weigold,[⊥] and D. A. Winkler[▽]

Contribution from the Departments of Chemistry and Physics, Flinders University of South Australia, G.P.O. Box 2100, Adelaide, SA 5001, Australia, Division of Information Technology, CSIRO, Swanston Street, Carlton, Victoria 3053, Australia, Institute für Physikalische and Theoretische Chemie, Technische Universität, D-38106, Braunschweig, Germany, Institute of Advanced Studies, R. S. Phys. S. E., Australian National University, Canberra, ACT 0200, Australia, and Division of Chemicals and Polymers, CSIRO, Private Bag 10, Clayton, Victoria 3168, Australia

Received August 30, 1996. Revised Manuscript Received November 25, 1996[⊗]

Abstract: An electronic structural study of the complete valence shell of [1.1.1]propellane is reported. Binding energy spectra were measured in the energy regime of 3.5−46.5 eV over a range of different target electron momenta, so that momentum distributions (MDs) could be determined for each ion state. Each experimental electron momentum distribution is compared with those calculated in the plane wave impulse approximation using both a triple-ζ plus polarization level SCF wave function and a further 13 basis sets as calculated using density functional theory. A critical comparison between the experimental and theoretical momentum distributions allows us to determine the optimum wave function for [1.1.1]propellane from the basis sets we studied. In general, the level of agreement between the experimental and theoretical MDs for this optimum wave function for all of the respective valence orbitals is fair. The determination of this wave function then allows us to derive the chemically interesting molecular properties of [1.1.1]propellane. A summary of these results and a comparison of them with those of other workers are presented with the level of agreement typically being good. In particular, we note that we confirm the existence of the C1−C3 bridging bond with a bond order of 0.70.

1. Introduction

Electron momentum spectroscopy (EMS), or (e,2e) coincidence spectroscopy, is now a well-developed tool for the investigation of the dynamic structure of molecules due to its unique ability to measure the orbital momentum profile for binding-energy-selected electrons.[1] Furthermore, within the plane wave impulse approximation (PWIA) and, in many cases, the target Hartree−Fock (THFA) approximation,[2,3] this measured momentum cross section may be directly compared with the calculated spherically averaged momentum distribution (MD) of a specific molecular orbital, once the appropriate angular-resolution function has been folded in.[4] Hence, EMS is also a powerful technique for evaluating the quality of theoretical wave functions in quantum chemistry,[5,6] and in this paper we report its application to the saturated hydrocarbon [1.1.1]propellane (C_5H_6).

The successful synthesis of [1.1.1]propellane,[7] a truly remarkable hydrocarbon with "inverted" geometries at the bridgehead carbon atoms, opened the way to both experimental and theoretical studies of its properties.[8] The structure,[9] vibrational spectrum,[10,11] total energy,[10] strain energy,[12] and heat of formation[10] have all been investigated. In addition, an excellent study into its low-energy electron impact spectroscopy has also been reported.[13] The compound was found to be remarkably stable and to have a surprisingly short bridgehead C1−C3 bond length (160 pm, of the order of only 9 pm longer than in cyclopropane), unexpected given the extreme deviation from tetrahedral geometry and the intuitively anticipated strain.

The above findings initiated a series of theoretical studies on the somewhat controversial nature of the C1−C3 bridging bond, a full description of which is found in Slee.[14] Briefly, however, attempts to describe the character of the bridging bond of [1.1.1]propellane have concentrated on two main lines of investigation. In the first, orbital theories were employed either to describe the bonding as predictive models on their own or as a means of analysing *ab initio* wave functions, while in the second the nature of the C1−C3 bond was studied using the electron density[15] or related quantities. In either approach, the fundamental questions being asked are is there in fact a bridging

[†] Department of Chemistry, Flinders University of South Australia.
[‡] Department of Physics, Flinders University of South Australia.
[§] Division of Information Technology, CSIRO.
[||] Institute für Physikalische and Theoretische Chemie.
[⊥] Australian National University.
[▽] Division of Chemicals and Polymers, CSIRO.
[⊗] Abstract published in *Advance ACS Abstracts,* March 1, 1997.
(1) McCarthy, I. E.; Weigold, E. *Rep. Prog. Phys.* **1991**, *54*, 789.
(2) McCarthy, I. E.; Weigold, E. *Rep. Prog. Phys.* **1988**, *51*, 299.
(3) Coplan, M. A.; Moore, J. H.; Doering, J. P. *Rev. Mod. Phys.* **1994**, *66*, 985.
(4) Frost, L.; Weigold, E. *J. Phys. B* **1982**, *15*, 2531.
(5) Bawagan, A.; Brion, C. E.; Davidson, E. R.; Feller, D. *Chem. Phys.* **1987**, *113*, 19.
(6) Zheng, Y.; Neville, J. J.; Brion, C. E. *Science* **1995**, *270*, 786.
(7) Wiberg, K. B.; Walker, F. H. *J. Am. Chem. Soc.* **1982**, *104*, 5239.
(8) Wiberg, K. B. *Acc. Chem. Res.* **1984**, *17*, 379.
(9) Hedberg, L.; Hedberg, K. *J. Am. Chem. Soc.* **1985**, *107*, 7257.
(10) Wiberg, K. B.; Dailey, W. P.; Walker, F. H.; Waddell, S. T.; Crocker, L. S.; Newton, M. *J. Am. Chem. Soc.* **1985**, *107*, 7247.
(11) Wiberg, K. B.; Rosenberg, R. E.; Waddell, S. T. *J. Phys. Chem.* **1992**, *96*, 8293.
(12) Wiberg, K. B.; Bader, R. F. W.; Lau, C. D. H. *J. Am. Chem. Soc.* **1987**, *109*, 1001.
(13) Schafer, O.; Allan, M.; Szeimies, G.; Sanktjohanser, M. *J. Am. Chem. Soc.* **1992**, *114*, 8180.
(14) Slee, T. S. In *Modern Models of Bonding and Delocalisation*; Liebman, J. F., Greenberg, A., Eds.; VCH Publishers: New York and Weinheim, 1988; p 63.
(15) Wiberg, K. B.; Bader, R. F. W.; Lau, C. D. H. *J. Am. Chem. Soc.* **1987**, *109*, 985.

S0002-7863(96)03058-2 CCC: $14.00

bond in [1.1.1]propellane, and if so, how can it be described and related to other bonds?

An orbital analysis of an *ab initio* wave function was performed by Jackson and Allen,[16] who focused on the valence canonical molecular orbitals and decomposed them using an interaction scheme between a C2 fragment and the outer parts of the rings (CH_2 groups). The highest-occupied molecular orbital (HOMO) was found to result from the in-phase combination of 2pσ orbitals on the bridgehead carbons, which has substantial density in the contributing regions. Jackson and Allen[16] claimed that this orbital "contributed nil to holding C1 to C3" and instead ascribed the bridgehead bonding to a degenerate pair of orbitals that place the electron density off-axis.

In an earlier paper, Newton and Schulman[17] noted that "the electron density in the interbridgehead region is little different from that in bicyclo[1.1.1]pentane, a compound in which no formal bridgehead−bridgehead bond exists". In addition, electron-density difference maps also appeared to support this conclusion, since they showed a region of charge depletion between the bridgehead carbons, just as they do for the bicyclo calculations.

The analysis of the total electron density obtained from *ab initio* calculations by Wiberg and co-workers[15,12] showed these descriptions to be misleading. Their results indicated three major conclusions including that there is a qualitative difference between the electron density in the bridging region of [1.1.1]-propellane and of the analogous bicyclic species, bicyclo[1.1.1]-pentane. The latter showed a minimum in the center of the region while the former showed a bond point.[14] Thus, in [1.1.1]-propellane there is a ridge of maximum electron density connecting the two carbon nuclei while in the bicyclic compound there is not. Hence, the bridgehead carbons are bonded in [1.1.1]propellane but are not in bicyclo[1.1.1]pentane. Their second major conclusion[12,15] was that there is also a quantitative difference between the electron density in the bridging region of [1.1.1]propellane and bicyclo[1.1.1]pentane. For instance, in [1.1.1]propellane the value of the electron density (ρ) at the bond point[15] is $\rho_b = 0.203\ a_0^{-3}$, while in bicyclo[1.1.1]pentane it is only[14] $\rho_b = 0.098\ a_0^{-3}$. We note at this time that Wiberg *et al.*[12,15] found the bond order[18] of [1.1.1]propellane to be $n = 0.73$. Finally, Wiberg *et al.*[12,15] found that the HOMO does contribute to the bonding of C1 and C3. Indeed they noted that roughly one-third of the total electron density at the bond point is due to the HOMO with its principal contribution, at this point, being due to the overlap of 2s orbitals. The assignment by Jackson and Allen[16] of the bonding as a result of off-axis density, and their claim that there is "very little charge density along the C1−C3 line of centers" is at variance with this observation of a bond point in the geometrical center of the [1.1.1]propellane molecule.

The nature of the hybridization of the C1−C3 bond in [1.1.1]-propellane has also been examined. In their earlier work, Newton and Schulman[17] found the hybridization of the inter-bridgehead bond to be $sp^{4.13}$. On the other hand in the more recent study of Jarret and Cusumano,[19] in which the $^{13}Cl-^{13}C2$ coupling constant in [1.1.1]propellane was measured to be 9.9 ± 0.1 Hz, the hybridization of the C1−C3 bridgehead bond was estimated to be $sp^{0.5}$.

The outer-valence structure of [1.1.1]propellane was previously studied with photoelectron spectroscopy (PES) using He-(I) radiation by Honegger *et al.*[20] In this work, five valence states were identified and classified, consistent with their expectation based on the results of the molecular orbital calculations[20] that assumed the validity of the Koopmans theorem, as being due to the respective $3a_1'$, $1e''$, $3e'$, $1a_2'$, and $2e'$ orbitals. We note that while no PES investigation of the inner valence $1a_2''$, $2a_1'$, $1e'$, and $1a_1'$ orbitals has been reported, there is our preliminary report[21] of some aspects of our investigations into [1.1.1]propellane which indicates binding energies and spectroscopic factors for the inner-valence orbitals. In addition, this work[21] confirmed the ordering of the outer-valence states as given by Honegger *et al.*[20] The molecular orbital nomenclature that we have adopted in this paper is consistent with that employed by Honegger *et al.*[20] in that the numbering of the symmetry labels within each irreducible representation refers to the valence-shell orbitals only (i.e., those of carbon 2s and 2p and hydrogen 1s parentage).

The only previous EMS study[21] into [1.1.1]propellane reported experimental binding energy spectra at two azimuthal angles, $\phi = 0°$ and 10° (see section 2) and the results of a Green's function calculation, to third order, in the algebraic diagrammatic construction (ADC(3)) method.

In section 2 we briefly discuss some of the experimental aspects of the EMS technique used in our work, while in section 3 details of our structure calculations are presented. In section 3 a brief discussion of the UniChem package and density functional theory (DFT) employed extensively in this investigation is provided. The results of the experimental and theoretical MDs are presented and discussed in detail in section 4. This is the first time these data have been reported in the literature for [1.1.1]propellane. The significance of the present application of the EMS technique to this molecule is that by comparing the experimental and theoretical MDs, for the relevant valence orbitals, we can independently determine which of the SCF or DFT basis sets of states we have studied provides the most physically reasonable representation of the [1.1.1]propellane molecule. Standard UniChem features then allow us to utilize this optimum wave function to extract the chemically important molecular property information for the [1.1.1]propellane system including bond lengths, bond orders, electron density (3D), and electron density contour (2D) plots and its infrared spectra. These data and a comparison with previous work are given and discussed in section 5 of this paper. Finally, in section 6, conclusions from the results of the present study are drawn.

2. Experimental Details

The EMS technique and its theoretical analysis have been discussed in detail elsewhere.[1] In the present work, noncoplanar symmetric kinematics is employed, with the two outgoing electrons, denoted by A and B, having essentially equal energies (500 eV) and making equal polar angles ($\theta = 45°$) with respect to the incident electron beam. The incident electron energy E_0 is 1000 eV plus the binding energy ϵ_f of the struck electron.

$$E_0 = E_A + E_B + \epsilon_f \tag{1}$$

The ion recoil momentum q (and thus the momentum p of the target electron) is varied by varying the out-of-plane azimuthal angle ϕ.

$$q = p_0 - p_A - p_B \tag{2}$$

At high enough energies and momentum transfer $|p_0 - p_A|$, momentum is transferred to the outgoing electrons only by a collision of the incident electron with a moving target electron of momentum p. In this case,[2]

(16) Jackson, J. E.; Allen, L. C. *J. Am. Chem. Soc.* **1984**, *106*, 591.
(17) Newton, M. D.; Schulman, J. M. *J. Am. Chem. Soc.* **1972**, *94*, 773.
(18) Bader, R. F. W.; Slee, T. S.; Cremer, D.; Kraka, E. *J. Am. Chem. Soc.* **1983**, *105*, 5061.
(19) Jarret, R. M.; Cusumano, L. *Tetrahedron Lett.* **1990**, *31*, 171.
(20) Honegger, E.; Huber, H.; Heilbronner, E.; Dailey, W. P.; Wiberg, K. B. *J. Am. Chem. Soc.* **1985**, *107*, 7172.
(21) Adcock, W.; Brunger, M. J.; Clark, C. I.; McCarthy, I. E.; Weigold, E.; Michalewicz, M. T.; Winkler, D. A.; von Niessen, W. *Chem. Phys. Lett.* **1995**, *244*, 433.

$$p = -q \tag{3}$$

The complete valence region of [1.1.1]propellane was studied in several experimental runs using the Flinders symmetric noncoplanar electron momentum spectrometer.[1,2] Both electron energy analyzers have position sensitive detectors in their energy-dispersing planes. A full description of the coincidence spectrometer and the method of taking the data can be found in McCarthy and Weigold,[1] although we note that since their report there has been a major upgrade in the data acquisition and computer control system. Specifically, the obsolete PDP-LSI 11/23 computer and its associated CAMAC control units were replaced by a PC 486D computer with a μ-ACE MCA card and a National Instruments LabPC+ card. The benefits of this upgrade in terms of data handling, processing, and storage and hardware reliability were manifest, in particular, by greatly reducing down time in the experiment.

In the current study, the binding energy range of interest ($\epsilon_f = 3.5-46.5$ eV for [1.1.1]propellane) is stepped through sequentially at each of a chosen set of angles ϕ using a binning mode[2] through the entire set of azimuthal angles ϕ. Scanning through a range of ϕ is equivalent to sampling different target electron momenta (see eqs 2 and 3) as

$$p = [(2p_A \cos\theta - p_0)^2 + 4p_A{}^2 \sin^2\theta \sin^2(^1/_2\phi)]^{1/2} \tag{4}$$

The energy resolution of the present work, as determined from measurements of the binding energy spectrum of helium, is 1.38 eV (fwhm). However, due to the natural line widths of the various transitions, as estimated from the relevant PES spectrum,[20] the fitted resolutions of the spectral peaks for [1.1.1]propellane varied from 1.42 to 2.60 eV (fwhm). The angular resolution was $\Delta\phi = 1.2°$, $\Delta\theta = 0.6°$, as determined from the electron optics and apertures and from a consideration of the argon 3p angular correlation. [1.1.1]Propellane of very high purity was introduced into the interaction region via a variable leak valve. The [1.1.1]propellane was prepared free of solvent from 1,3-diiodobicyclo[1.1.1]pentane by a procedure outlined by Alber and Szeimies,[22] although we note that the original synthesis of [1.1.1]-propellane was due to Wiberg and Walker.[7] Since the EMS technique is very sensitive to impurities, great care was exercised to minimize the possibility of sample contamination both during its synthesis and in its transportation from the storage reservoir to the interaction region. With regard to the latter point, the [1.1.1]propellane sample was always initially condensed by liquid N_2 and any N_2, O_2, H_2O, etc., contaminants pumped off. The sample was kept at 15 °C and its vapor introduced through a 0.7 mm diameter single capillary into the interaction region. Note that the [1.1.1]propellane driving pressure was too low to cause any significant clustering by supersonic expansion. Since we were unsure as to the long-term stability of gas phase [1.1.1]propellane, and indeed how it interacts with the walls of its storage reservoir and stainless steel gas transport lines, the results of each scan were carefully monitored for any signs of sample degradation. Furthermore, our [1.1.1]propellane samples were regularly changed to additionally minimize the possibility of sample degradation.

3. Theoretical Analysis

The PWIA is used to analyze the measured cross sections for high-momentum transfer (e,2e) collisions.[2] Using the Born−Oppenheimer approximation for the target and ion wave functions, the (e,2e) differential cross section σ, for randomly-oriented molecules and unresolved rotational and vibrational states, is given by

$$\sigma = K\int d\Omega\ |\langle p\Psi_f{}^{N-1}|\Psi_i{}^N\rangle|^2 \tag{5}$$

where K is a kinematical factor which is essentially constant in the present experimental arrangement, $\Psi_f{}^{N-1}$ and $\Psi_i{}^N$ are the electronic many-body wave functions for the final (($N-1$) electron) ion and target (N electron) ground states, and p is the momentum of the bound electron at the instant of ionization. The $\int d\Omega$ denotes an integral over all angles (spherical averaging) due to the averaging over all initial rotational states. The average over the initial vibrational state is well approximated by evaluating orbitals at the equilibrium geometry of the molecule. Final rotational and vibrational states are eliminated by closure.

The momentum-space target-ion overlap[23] $\langle p\Psi_f{}^{N-1}|\Psi_i{}^N\rangle$ can be evaluated using configuration interaction (CI) descriptions of the many-body wave functions, but usually the weak-coupling approximation[1] is made. Here, the target-ion overlap is replaced by the relevant orbital of, for example, the Hartree−Fock or Kohn−Sham[24] ground state Φ_i, multiplied by a spectroscopic amplitude, which is the coefficient, in the CI description of the ion state, of the configuration representing a hole in the appropriate ground state orbital. With these approximations, eq 5 reduces to

$$\sigma = KS_j^{(f)}\int d\Omega\ |\phi_j(p)|^2 \tag{6}$$

where $\phi_j(p)$ is the momentum space orbital. The spectroscopic factor $S_j^{(f)}$ is the square of the spectroscopic amplitude for orbital j and ion state f. It satisfies the sum rule

$$\sum_f S_j^{(f)} = 1 \tag{7}$$

Hence, it may be considered as the probability of finding the one-hole configuration in the many-body wave function of the ion.

The target-ion overlap is a one-electron function called the quasiparticle orbital. A quasiparticle equation, the Dyson equation, can be constructed from the electronic Schrödinger equations for the target and ion.[23] Formally this is a one-electron Schrödinger equation with target and ion structure details contained in the potential operator. The quasiparticle energies are given by the poles in the Greens function of this equation, which can be evaluated using diagrammatic perturbation theory.[25] An example of this calculation, which omits diagrams above the third order, is the third-order algebraic diagrammatic construction, or ADC(3), method.

The Kohn−Sham equation[24] of DFT may be considered as an approximate quasiparticle equation, with the potential operator approximated by the exchange-correlation potential.[23] Recently,[26] the physical significance of the valence orbitals of DFT has been shown by their ability to describe EMS data that are not well described by SCF calculations that omit electron-correlation considerations, but are well described by full CI calculations.

In order to compute the coordinate-space Kohn−Sham orbitals ψ_j, we employed DGauss, a program developed for CRAY Research by Andzelm and co-workers.[27,28] DGauss is itself a part of UniChem, a suite of computational quantum-chemistry programs from CRAY Research Inc.[29] Using DGauss and UniChem, we employed various basis sets to build a model [1.1.1]propellane molecule and then we minimized the energy. The molecular coordinates at the optimum geometry (minimum energy) and the Gaussian molecular orbital parameters (coefficients and exponents) were next treated as an input to the Flinders-developed program AMOLD, which computes the momentum space spherically-averaged molecular-structure factor[30] and the (e,2e) cross section or momentum profile.

The comparisons of calculated momentum profiles with experiment (see section 4) may be viewed as an exceptionally-detailed test of the quality of the basis set. In this study, we have used thirteen basis sets in the DFT (DGauss) computations (Table 1). The notations DZ and TZ denote basis sets of double-, or triple-ζ quality. V denotes a calculation in which such a basis is used only for the valence orbitals

(22) Alber, F.; Szeimies, G. *Chem. Ber.* **1992**, *125*, 757.
(23) Casida, M. *Phys. Rev. A* **1995**, *51*, 2005.
(24) Kohn, W.; Sham, L. J. *Phys. Rev.* **1965**, *140*, A1133.
(25) von Niessen, W.; Schirmer, J.; Cederbaum, L. S. *Comput. Phys. Rep.* **1984**, *1*, 58.
(26) Duffy, P.; Chong, D. P.; Casida, M.; Salahub, D. R. *Phys. Rev. A* **1994**, *50*, 4707.
(27) Andzelm, J.; Wimmer, E. *J. Chem. Phys.* **1992**, *96*, 1290.
(28) Komornicki, A.; Fitzgerald, G. *J. Chem. Phys.* **1993**, *98*, 1398.
(29) UniChem Chemistry Codes; APG-5505 3.0; CRAY Research, Inc., Mendota Heights; pp 145−190.
(30) Michalewicz, M. T.; Brunger, M. J.; McCarthy, I. E.; Norling, V. M. In *CRAY Users Group 1995 Fall Proceedings*; Shaginaw, R., Ed.; Alaska, 1995; pp 37−41.

Table 1. Basis Sets Used in the Present Study for the DGauss Computations

Pople sets	3-21G	4-31G*	6-31G	6-31G*	6-311G	6-311G*	
DGauss sets	DZ94	DZ94p	DZVP	DZVP2	TZ94	TZ94p	TZVP

Table 2. Local Spin-Density-Optimized Basis Sets Used in the DGauss Computations

atom	DZ94	DZ94p	DZVP	DZVP2	TZ94	TZ94p	TZVP
H	(41)	(41)	(41)	(41/1)	(311)	(311/1)	(3111/1)
C	(621/41)	(621/41/1)	(621/41/1)	(721/51/1)	(7111/411)	(7111/411/1)	(7111/411/1)

and a minimal basis is used for the less-chemically-reactive orbitals. The inclusion in the basis of long-range polarization functions is denoted by P.

Table 2 lists the basis sets available in DGauss for hydrogen and carbon atoms. We used all of them in our studies of [1.1.1]propellane. The notation indicates the number of primitive Gaussians and the contraction scheme. For example, (621/41/1) means there are 3 contracted s, 2 contracted p, and 1 contracted d functions. The s functions consist of 6, 2, and 1 primitive Gaussians while the p functions consist of 4 and 1 primitive Gaussians. An improvement over the local-density approximation (LDA) or the local-spin-density (LSD) approach to approximating the exchange-correlation functional can be obtained by using functionals that depend upon the gradient of the charge density.[31−38] In our study, we used two different approximations to the exchange-correlation energy functional due to Becke and Perdew[31−33] (basis sets marked bp) and Becke, Stoll, Pavlidou, and Preuss[31,32,34] (basis sets marked bspp). The nonlocal density-gradient correction for the above two nonlocal models, as implemented in DGauss, was applied after the final self-consistent energy-optimization step.

For comparison with the DFT orbitals, we used SCF orbitals computed by GAMESS[39] using Dunning[40] basis sets at the triple-ζ-plus-polarization level. This calculation used the optimized structural geometry of Wiberg.[41]

The results presented in the next section illustrate the quality of each of the orbitals. However, for the sake of clarity, not all of the results from the basis sets we investigated could be plotted in the figures presented in the next section, so that only a subset of these results from our 13 basis sets are in fact given. In this regard, we have exercised our judgement as to which illustrate a pertinent physical point.

4. Comparison between Experimental and Theoretical Momentum Distributions

Typical binding energy spectra of C_5H_6 in the region of 3.5−46.5 eV and at a total energy of 1000 eV are given in Figure 1. These spectra were measured at each of a chosen set of angles ϕ and then analyzed with a least-squares-fit deconvolution technique.[42] This analysis then allowed us to derive the required momentum distributions for the respective valence states of [1.1.1]propellane. Although the measured momentum distributions are not absolute, relative magnitudes for the different transitions are obtained.[1] In the current EMS investigation of the valence states of C_5H_6, the experimental momentum distributions are placed on an absolute scale by summing the experimental flux for each measured ϕ (or, as we saw from eq 4, p) for the first four ($3a_1'$, $1e''$, $3e'$, and $1a_2'$ states) outer-valence states, and then normalizing this to the corresponding sum from the result of our PWIA-DFT TZ94.bspp calculation.

In Figure 2 we compare our experimental momentum distribution for the highest-occupied molecular orbital (HOMO), $3a_1'$ state (peak 1 of Figure 1) at $\epsilon_f = 9.7$ eV, of C_5H_6 with a small selection of the results from our PWIA-SCF and PWIA-DFT calculations. We note that the errors on all the present momentum distributions, as derived during the deconvolution procedure, are two standard deviation uncertainties, thus implying a 95.4% confidence limit.[42] It is clear from Figure 2 that the measured momentum distribution for the $3a_1'$ state is strongly peaked at smaller values of p, thus implying that this HOMO is s-like in nature. All of the theoretical PWIA-SCF and PWIA-DFT results are consistent with this observation, although it is also apparent from Figure 2 that the 6-31G Pople basis results in a momentum distribution which seriously underestimates the measured (e,2e) cross section at small p. On the other hand, both the TZ94p.bp and TZ94p.bspp basis sets (not plotted) lead to a calculated (e,2e) cross section which is too large, compared to the experimental result, at small values of p ($\approx$0.16 au). The MD result for the remaining DFT basis set, which we specifically plotted in Figure 2, is in fair accord with the experimental result. Finally, we note that if the result of the present PWIA-DFT calculation for the TZ94.bspp basis is scaled by our previously determined ADC(3) level spectroscopic factor[21] for the $3a_1'$ state at $\epsilon_f \approx 9.7$ eV, $S_{3a_1'}^{ADC(3)} = 0.89$, then the level of agreement between the experimental and theoretical momentum distributions is now good (see Figure 2).

For the next outermost valence $1e''$ state (peak 2 of Figure 1) at $\epsilon_f = 11.3$ eV, the level of agreement between the theoretical and experimental MDs is generally quite poor. Here (Figure 3) we find our PWIA-SCF result and that our PWIA-DFT results, with 6-31G Pople, TZ94p.bp, TZ94p.bspp, and DZ94 basis sets of states, lead to momentum distributions that underestimate the strength of the (e,2e) cross section for $p <$ 0.6 au and overestimate it thereafter. The outstanding exceptions to this are the results of our PWIA-DFT calculations with the TZ94 and TZ94.bspp basis sets. In this case (see Figure 3), their level of accord with the experimental MD data for the $1e''$ state is excellent for $p <$ 0.6 au and $p >$ 1.4 au. However, for the momentum range 0.6 au $< p <$ 1.4 au, we note that the (e,2e) cross section, as calculated using the TZ94 and TZ94.bspp basis sets, is somewhat stronger in magnitude than that observed experimentally, suggesting that there remain some limitations with these basis states. Figure 3 thus indicates that for the theory to reproduce correctly the momentum distribution for the $1e''$ state both a quite sophisticated triple-ζ basis set[43] and the incorporation of electron correlation effects via the exchange-correlation potential of DFT are required. This is an interesting result since while these electron correlation effects are very important in small molecules such as water[5] and ammonia,[44] they have not previously been demonstrated to be of significance in hydrocarbons.[44] We note at this time that since the PWIA-

(31) Becke, A. D. *Phys. Rev. A.* **1988**, *38*, 3098.
(32) Becke, A. D. *J. Chem. Phys.* **1988**, *88*, 2547.
(33) Perdew, J. P. *Phys. Rev. B.* **1986**, *33*, 8822.
(34) Stoll, H.; Pavlidou, C. M. E.; Preuss, H. *Theor. Chim. Acta* **1978**, *49*, 143.
(35) Lee, C.; Parr, R. G.; Yang, W. *Phys. Rev. B.* **1988**, *37*, 785.
(36) Dunlap, B. I.; Connolly, J. W. D.; Sabin, J. R. *J. Chem. Phys.* **1979**, *71*, 3396; **1979**, *71*, 4993.
(37) Levy, B. *Chem. Phys. Lett.* **1969**, *4*, 17.
(38) Jorgensen, P.; Linderner, J. *Int. J. Quantum Chem.* **1970**, *4*, 587.
(39) Schmidt, M.; Baldridge, K. K.; Boatz, J. A.; Jensen, J. H.; Koseki, S.; Gordon, M.; Nguyen, K. A.; Windurs, T. L.; Elbert, S. T. *QCPE Bull.* **1984**, *14*, 52.
(40) Dunning, T. H. *J. Chem. Phys.* **1971**, *55*, 716.
(41) Wiberg, K. *J. Am. Chem. Soc.* **1983**, *105*, 1227.
(42) Bevington, P. R.; Robinson, D. K. *Data Reduction and Error Analysis for the Physical Sciences*; McGraw-Hill, Inc.: New York, 1990.
(43) Dunning, T. H. *J. Chem. Phys.* **1989**, *90*, 1007.
(44) Brion, C. E. In *The Physics of Electronic and Atomic Collisions*; Anderson, T., Fastrup, B., Folkmann, F., Knudsen, H., Andersen, N., Eds.; American Institute of Physics: New York, 1993; p 350.

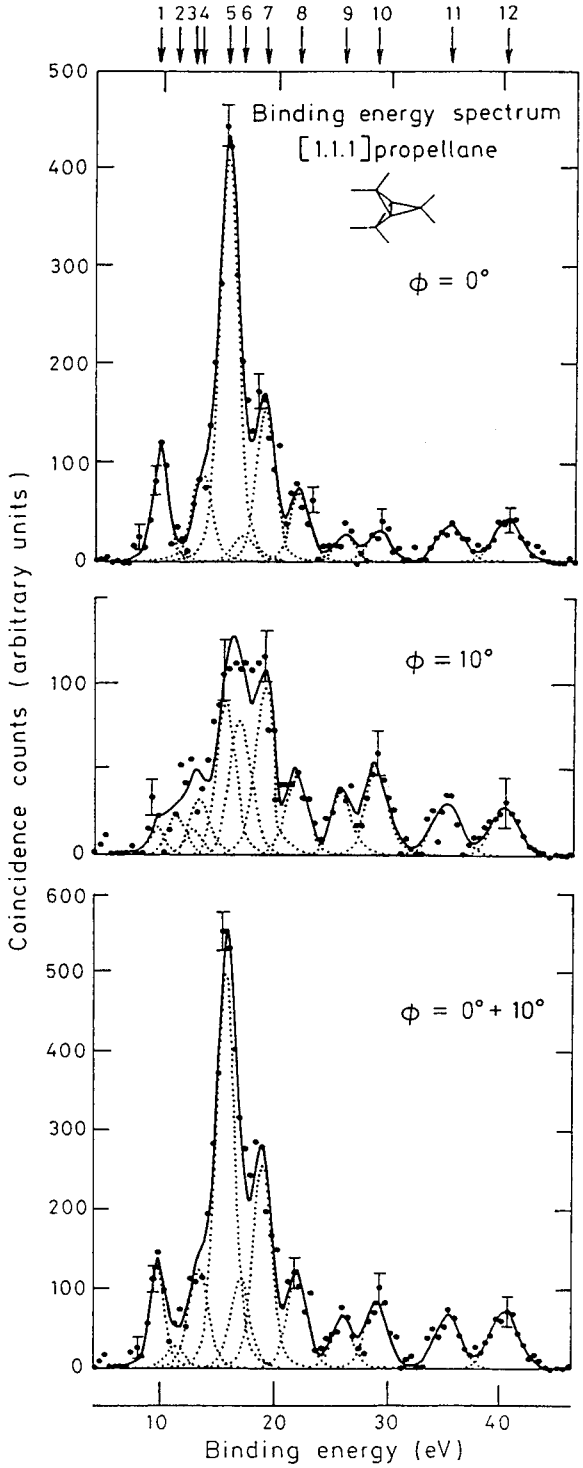

Figure 1. Typical binding energy spectra from our 1000 eV noncoplanar symmetric EMS investigation into [1.1.1]propellane. The curves show the fits to spectra at $\phi = 0°$, $\phi = 10°$, and $\phi = 0° + 10°$ using the known energy resolution function. We thank Elsevier Science for permission to reproduce this figure from ref 21.

DFT result with the TZ94.bspp basis is only marginally in better agreement with the experimental momentum distribution than that obtained with the TZ94 basis, we can infer that in this case the more exact nonlocal exchange-correlation functionals afforded by the Becke−Stoll−Preuss−Pavlidou corrections are not really necessary.

The 3e′ state at a binding energy of 12.6 eV and the $1a_2'$ state at a binding energy of 13.4 eV are only separated by 0.8 eV. Consequently, given our coincident energy resolution of $\Delta E_{coin} = 1.38$ eV (fwhm), we were not confident of uniquely resolving them in our deconvolution of the measured spectra.

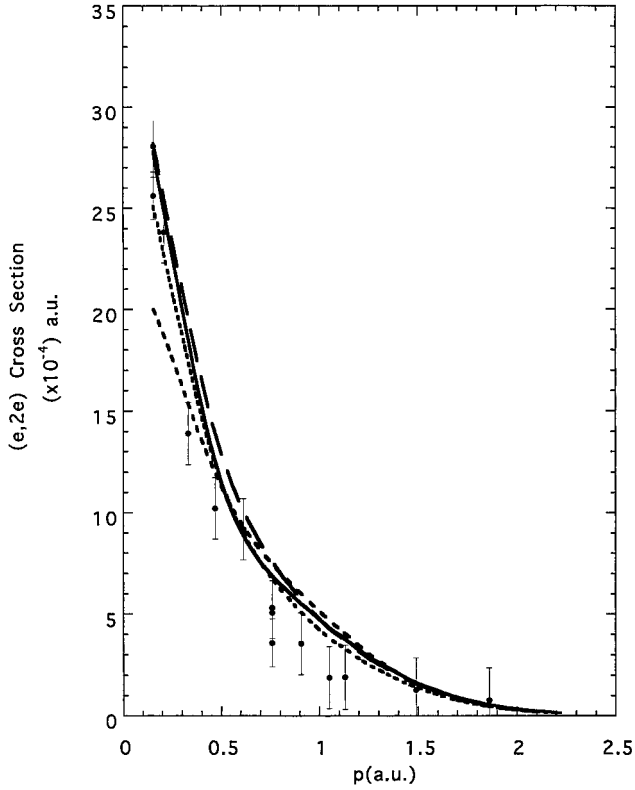

Figure 2. The 1000 eV noncoplanar symmetric momentum distribution for the $3a_1'$ state of [1.1.1]propellane. The present data (●) are compared against the results of our PWIA-SCF triple-ζ basis (—), PWIA-DFT 6-31G Pople basis (- - -), and PWIA-DFT TZ94.bspp basis (− − −) calculations. Also shown is the result of the PWIA-DFT TZ94.bspp basis (- - - - - - -) scaled by a factor of 0.89.

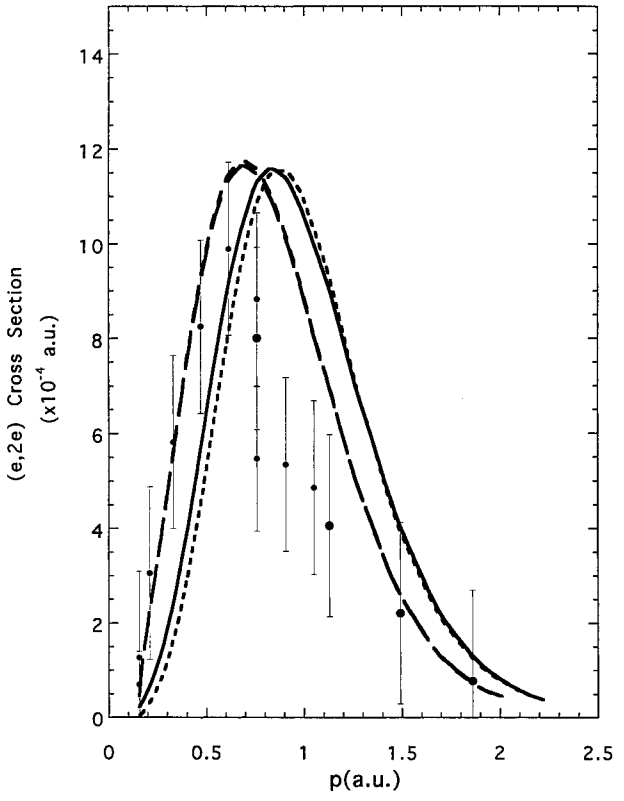

Figure 3. The 1000 eV noncoplanar symmetric momentum distribution for the 1e″ state of [1.1.1]propellane. Legends are the same as in Figure 2. Also shown is the result of our PWIA-DFT TZ94 basis (− − −).

Thus, a combined momentum distribution for the 3e′ and $1a_2'$ states (peaks 3 and 4 of Figure 1) is presented in Figure 4. If we now consider Figure 4 in more detail, then it is clear that

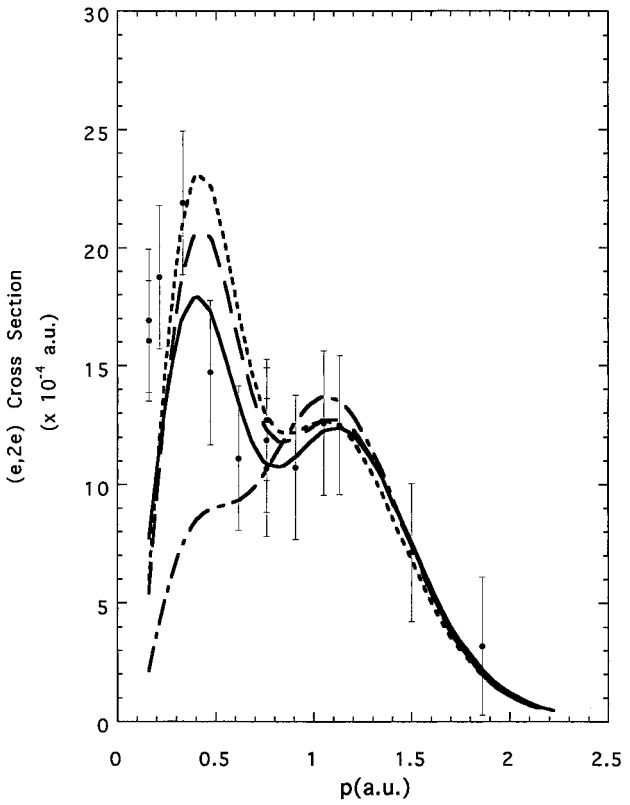

Figure 4. The 1000 eV noncoplanar symmetric momentum distribution for the $3e' + 1a_2'$ states of [1.1.1]propellane. Legends are the same as in Figure 2. Also shown is the result of our PWIA-DFT TZ94p.bspp basis (− - −).

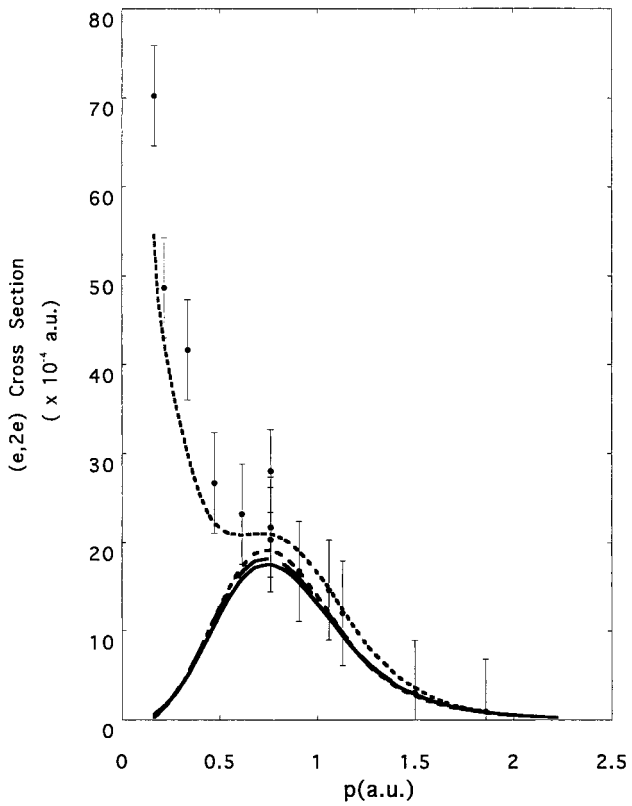

Figure 5. The 1000 eV noncoplanar symmetric momentum distributions for the $2e'$ state of [1.1.1]propellane. Legends are the same as in Figure 2. Also shown is the result for the PWIA-DFT TZ94.bspp basis (- - - - - - -) when a $(0.55)2a_1'$ pole strength contribution is added to that for the $2e'$ state.

none of our PWIA-SCF and PWIA-DFT calculations exactly reproduce the measured MD. In particular the TZ94p.bp (not plotted) and TZ94p.bspp basis sets lead to momentum distributions which completely fail to predict the first peak in the measured (e,2e) cross section, strongly suggesting that they are totally inadequate in providing a realistic physical picture for these states. With regard to the remaining basis sets, while they all lead to a quite good qualitative representation of the measured momentum distribution, there are differences in some of the fine details between them and the experimental cross section. Specifically the PWIA-SCF and PWIA-DFT results, with 6-31G Pople, TZ94, DZ94, and TZ94.bspp basis sets, all predict the first peak in the $3e' + 1a_2'$ cross section to occur at a value of momentum $p \approx 0.40$ au, which is too large compared to our experimental observation for this peak of $p \approx 0.33$ au. The additional experimental flux at small momentum, compared to the theoretical results, suggests that the orbitals for the $3e' + 1a_2'$ states are somewhat more diffuse in coordinate space than those afforded by the basis states considered in this investigation. Nonetheless we consider that, across the current experimental range of momentum, the present PWIA-DFT results using the respective 6-31G Pople and TZ94.bspp basis sets provide a fair level of agreement with the measured data for the $3e' + 1a_2'$ states.

In Figure 5 we plot the experimental momentum distribution for the $2e'$ orbital (peak 5 of Figure 1), at binding energy $\epsilon_f =$ 15.7 eV, along with our theoretical PWIA-SCF and PWIA-DFT results. It is quite clear from this figure that none of the calculations, for any of the basis sets considered, provides an (e,2e) cross section in agreement with the experimental result. This is particularly apparent for momenta less than 0.76 au, where the measured cross section starts to increase in value until reaching a maximum at $p \approx 0.16$ au (i.e., it is s-like in nature), while all of the theoretical cross sections tend to 0 as p approaches 0.16 au (i.e., they are all p-like in nature). For $p >$ 0.76 au, we see from Figure 5 that, to within the errors on the momentum distribution data, there is fair agreement between all the $2e'$ orbital PWIA-SCF and PWIA-DFT calculation results and the experiment, although it is perhaps interesting to note that the magnitude of the measured data still lay above the theoretical cross section for all $p > 0.76$ au. In Adcock *et al.*,[21] we previously noted that our ADC(3) calculation found that the $2a_1'$ orbital was severely split, with a significant $2a_1'$ pole strength ($S_{2a_1'}^{ADC(3)} = 0.39$) at almost the same binding energy as that of the $2e'$ orbital. We further noted in Adcock *et al.*[21] that some evidence in support of that prediction was provided by the PES spectrum of Honegger *et al.*[20] who found that peak 5 in their spectrum was quite asymmetric. If we now allow for some $2a_1'$ flux in our PWIA-DFT calculation (55% contribution allowed here) using the TZ94.bspp basis, then very good qualitative agreement is found between theory and experiment for this combined momentum distribution. This is well illustrated by our plot in Figure 5 for the $2e' + (0.55)2a_1'$ states MD. Obviously the level of agreement for the (e,2e) cross section, between the theory result that incorporates a $2a_1'$ contribution to the $2e'$ state and the measured data, is not perfect, perhaps reflecting a limitation in our $2a_1'$ orbital. Nonetheless this agreement is still quite good with the present analysis providing the first unequivocal supporting evidence for the ADC(3) $2a_1'$ orbital spectroscopic strength splitting result of Adcock *et al.*[21]

If we now consider the $1a_2''$ state (peak 6 of Figure 1), then the level of agreement between the present experimental momentum distribution and the MDs from the results of the PWIA-SCF and PWIA-DFT calculations, with the respective 6-31G Pople basis, TZ94 basis, TZ94.bspp basis, and DZ94 basis, is excellent across the entire range of measured momentum (see Figure 6). Both the experimental MD and these theoretical MDs accurately predict that the peak in the $1a_2''$ cross

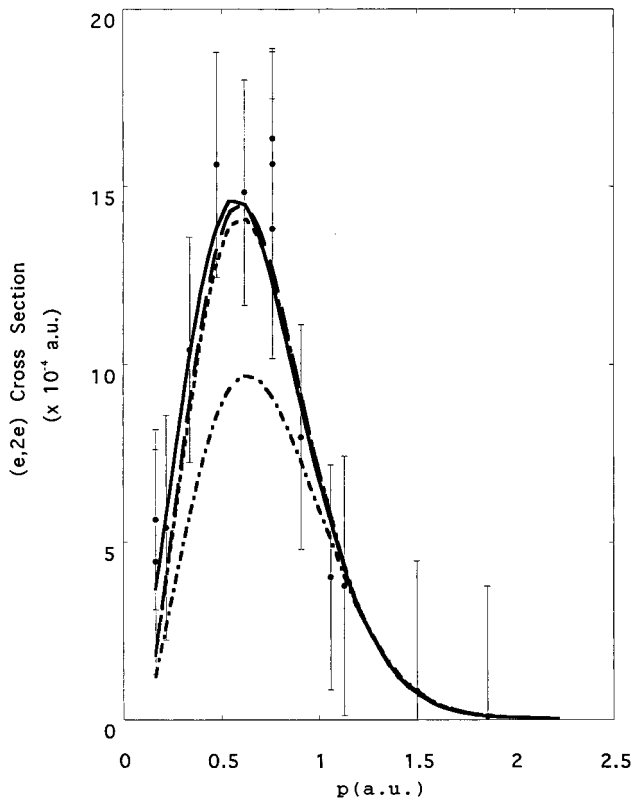

Figure 6. The 1000 eV noncoplanar symmetric momentum distribution for the $1a_2''$ state of propellane. Legends are the same as in Figure 2. Also shown is the result of our PWIA-DFT TZ94p.bp basis (− - − - −).

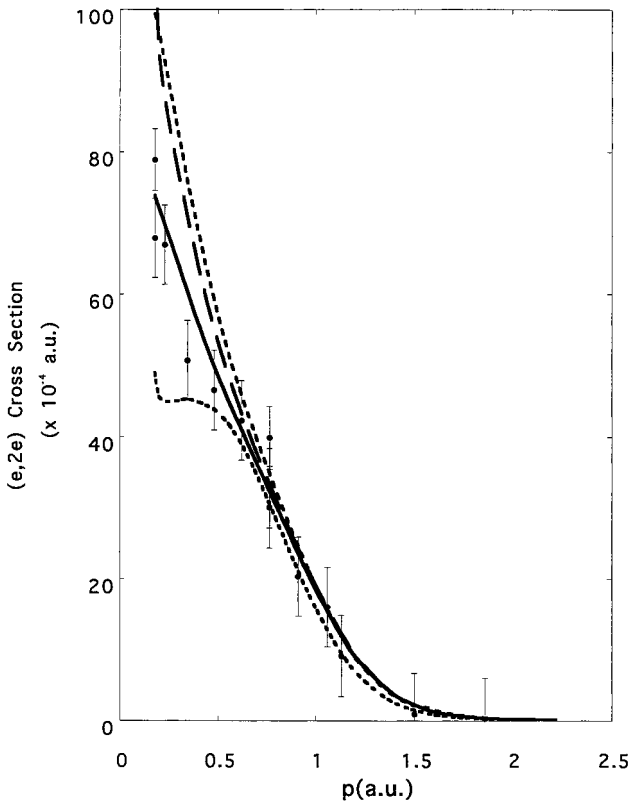

Figure 7. The 1000 eV noncoplanar symmetric distribution for the $2a_1' + 1e'$ states of [1.1.1]propellane. Legends are the same as in Figure 2. Also shown is the result for the PWIA-DFT TZ94.bspp basis (- - - - - - -) when only a $(0.43)2a_1'$ pole strength contribution is added to that for the $1e'$ state.

section occurs at a momentum $p \approx 0.62$ au. The PWIA-DFT results with TZ94p.bp and TZ94p.bspp (not plotted) basis states also predict that the peak in this cross section occurs at $p \approx 0.62$ au, but they significantly underestimate the magnitude of the (e,2e) cross section at the peak (∼33% too small in magnitude). This result adds further weight to what we have previously observed for the $1e''$ state and the $3e' + 1a_2'$ states, that the TZ94p.bp and TZ94p.bspp bases are not providing a very realistic description for the [1.1.1]propellane wave function.

The ADC(3) level calculation of Adcock *et al.*[21] found that both of the inner-valence $2a_1'$ and $1e'$ orbitals were significantly split into poles of important spectroscopic strength. Furthermore, these poles were also observed, in terms of the binding energies at which they are located, to intermix. Consequently 4 Gaussians (peaks 7−10 of Figure 1) were required to represent all the measured flux of these orbitals, and due to the aforementioned intermixing of $2a_1'$ and $1e'$ intensities, we can only report momentum distributions for the sum of those states (i.e., MDs for $2a_1' + 1e'$). In Figure 7 we therefore plot the present experimental momentum distribution for the $2a_1' + 1e'$ states. Also included in this figure are the results from our PWIA-SCF and PWIA-DFT calculations. We again find that the shapes of the MDs from the PWIA-DFT calculations, with TZ94p.bp and TZ94p.bspp basis sets, are not in good accord with that observed experimentally. On the other hand, the shapes of the cross sections for both the PWIA-SCF and PWIA-DFT calculations, with 6-31G Pople basis, DZ94 basis (not plotted), TZ94 basis (not plotted), and TZ94.bspp basis, are all in good accord with that measured experimentally (see Figure 7). Indeed, the magnitude of the present PWIA-SCF calculation, using a triple-ζ level basis, is in good agreement for all p with the measured MD for the $2a_1' + 1e'$ cross section, although as we shall shortly see this agreement is probably fortuitous. We note, however, that the four remaining PWIA-DFT results overestimate the magnitude of the cross section for $p < 0.5$ au.

This result is in itself not alarming if we recall that the ADC(3) calculation predicted a pole strength for the $2a_1'$ orbital, at the binding energy $\epsilon_f = 19.07$ eV (i.e., within the binding energy region encompassed by peaks 7−10 of Figure 1), to be only $S_{2a_1'}^{ADC(3)} = 0.43$. Hence, on this basis, we should *a priori* expect the full PWIA-DFT $2a_1' + 1e'$ momentum distribution to overestimate the magnitude of the measured cross section, particularly at small values of p where the $2a_1'$ contribution dominates, which is exactly what we see in Figure 7. If we now consider the theoretical MD which results when only a 43% $2a_1'$ contribution is added to the $1e'$ cross section, in particular within the PWIA-DFT framework for a TZ94.bspp basis, then the level of agreement between the experimental MD and the $(0.43)2a_1' + 1e'$ PWIA-DFT MD is generally quite good, the exception being at values of momenta $p < 0.35$ au. This lack of agreement between the calculated MD for $(0.43)2a_1' + 1e'$ and the experimental MD at small values of p is possibly indicative of a limitation of the current $2a_1'$ orbital in the TZ94.bspp basis. Alternatively, it is also possible that there is some $1a_1'$ flux under peaks 7−10 of Figure 1 which we have not accounted for. Certainly the ADC(3) result of Adcock *et al.*[21] shows that the $1a_1'$ orbital spectroscopic strength is severely split among numerous poles. Thus, the possibility of about a 20% $1a_1'$ contribution to the measured MD can not be discounted here.

The innermost-valence $1a_1'$ state is seen to be severely split among many poles, consistent with the ADC(3) result of Adcock *et al.*,[21] due to final state correlation effects so that two rather broad Gaussians (peaks 11 and 12 of Figure 1) were needed to fit the observed spectral strength for $\epsilon_f \geq 31.5$ eV. Comparing our experimental MD to those calculated within the PWIA-SCF and PWIA-DFT frameworks, it is then apparent from Figure 8 that all the calculations overestimate the magnitude of the (e,2e)

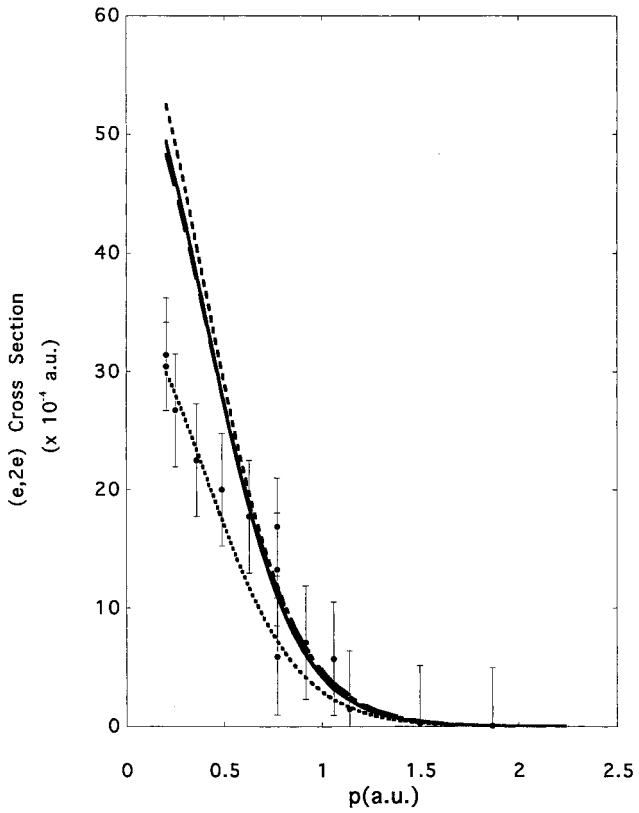

Figure 8. The 1000 eV noncoplanar symmetric momentum distribution for the $1a_1'$ state of [1.1.1]propellane. Legends are the same as in Figure 2. Also shown is the result for the PWIA-DFT TZ94.bspp basis (- - - - - - -) scaled by a factor of 0.62.

cross section for the $1a_1'$ state. However, when the theory results are scaled by a factor of 0.62, in particular Figure 8 for the specific case of (0.62)PWIA-DFT TZ94.bspp, the level of agreement between the measured MD and this calculation is now excellent for all p. This missing 38% $1a_1'$ intensity might be located at binding energies not accessed in the present measurements (ϵ_f > 46.5 eV) or, at least in part, under peaks 7−10 of Figure 1 (see the above discussion). In any event, this highlights how difficult it can be to interpret the measured momentum distribution data for the inner-valence region when the spectroscopic strength of the states is severely split into many poles.

In summary, the above extensive comparison between our experimental and theoretical MDs, for all of the valence electronic states of [1.1.1]propellane, leads us to conclude that of the basis states we investigated, the DFT TZ94.bspp provides the most physically-realistic description for the [1.1.1]propellane wave function. While we concede the result of our PWIA-DFT TZ94.bspp calculations are not in perfect agreement with the corresponding measured MDs, indicating there are some limitations with this basis, they are nonetheless in fair agreement with them. Consequently, in the next section of this paper, we utilize this optimum wave function to determine some of the chemically interesting molecular property information for [1.1.1]-propellane.

5. Molecular Property Information

Experimental validation of density functional basis sets using EMS may provide a route to optimum basis sets for other types of molecular properties, such as molecular geometries, bond orders, charge distributions, and orbital energies. Previous work[8−19] has used a variety of molecular orbital approaches to determine structural and electronic properties of [1.1.1]propellane.

Our calculations using the optimum TZ94.bspp basis set gave good agreement between experimentally-determined molecular properties and compared favorably with the results from other MO calculations. In particular, the interbridgehead carbon−carbon distance was 1.59 Å, in excellent agreement with the experimental value of 1.596 Å. The DFT calculations indicated considerable negative charge on the methylene carbons (Mulliken net atomic charge of −0.538, Löwdin net atomic charge of −0.265) with the bridgehead carbons remaining essentially neutral (Mulliken net atomic charge of −0.016, Löwdin net atomic charge of −0.093). The results are summarized in Table 3.

From the DFT calculations we were also able to calculate the frequencies of the vibrational modes of [1.1.1]propellane with reasonable accuracy. In addition, the calculated intensities of the transitions are in reasonable agreement with the observed experimental infrared spectrum of [1.1.1]propellane.[10] The main discrepancy is with the intensity of the CH stretching vibrations near 3000 cm^{-1}, which are predicted to be weaker than observed. Other theoretical work on the vibrational spectrum of [1.1.1]propellane includes the 6-31G*MP2 calculations of Riggs *et al.*[45] which yielded excellent agreement with experiment and useful predictions of the properties and stability of the sulfur analogue, trithia[1.1.1]propellane.[45]

It is of particular interest to investigate the electron density in the interbridgehead region of [1.1.1]propellane. We performed a study analogous to that of Wiberg,[12,15] to estimate the electron density (ρ) at the bond critical point[15] (midway between the two bridgehead carbons). We obtained a value of $\rho_b = 0.173\ a_0^{-3}$, compared to the Wiberg value of $0.203\ a_0^{-3}$. We then used the Wiberg empirical method to calculate bond orders from electron densities at the bond critical points derived from the TZ94.bspp basis calculations. The relation between the bond order n and the bond critical point electron densities ρ_b[15] is

$$n = \exp[7.004(\rho_b - 0.224)] \qquad (8)$$

This relationship yielded a bond order for the interbridgehead bond in [1.1.1]propellane of 0.70, very similar to the Wiberg value[15] of 0.73. We also calculated the bond order of the interbridgehead bond using Mulliken and Mayer populations analysis. The Mayer bond order of 0.55 was in reasonable agreement with our value of 0.70. The Mulliken value of −0.11 reflects the well-known deficiencies of this method of orbital decomposition.

In order to assess the claim of Newton and Schulman[17] that the electron density in the interbridgehead region of [1.1.1]-propellane is little different from that in bicyclo[1.1.1]pentane, we also calculated the electron density and bond order for the latter compound using the same basis set and nonlocal functional as the [1.1.1]propellane calculations. We obtained a value of $0.097\ a_0^{-3}$ for the electron density midway between the bridgehead carbon atoms of bicyclo[1.1.1]pentane, very similar to the value of $0.098\ a_0^{-3}$ reported by Wiberg. The bond order from the above empirical relationship (see eq 8) for bicyclo-[1.1.1]pentane was 0.40 (for this relationship zero electron density gives a bond order of 0.21), indicating little or no interbridgehead bond in this compound. Mayer population analysis from our DFT calculation of bicyclo[1.1.1]pentane yielded a bond order of 0.075, again consistent with negligible bonding between the bridgehead carbons and markedly different to the value of 0.55 for [1.1.1]propellane.

The present experiment and its analysis contribute to the understanding of the bonding between the bridgehead carbon

(45) Riggs, N. V.; Zoller, U.; Nguyen, M. T.; Radom, L. *J. Am. Chem. Soc.* **1992**, *114*, 4354.

Table 3. A Comparison between the Present Results and the Results of Other Calculations and Experiments for Some of the Important Molecular Properties of [1.1.1]Propellane

	experimental		theoretical						
property[a]	IR[10]	ED[9]	TZ94.bspp this work	6-31G* [14]	6-31G*-MP2[11]	6-31G*-MP2[10]	6-311G(MC)-MP2[45]	6-31G*-MP2[45]	6-31G*-MP3[10]
$r(C_b-C_n)$, Å	1.522 ± 0.002	1.525 ± 0.002	1.518	1.502	1.514	1.515	1.521	1.525	1.514
			1.522						
			1.523						
			1.531						
			1.529						
			1.526						
			1.525 ± 0.004[b]						
$r(C_b-C_b)$, Å	1.60 ± 0.02	1.596 ± 0.005	1.586	1.543		1.594	1.602	1.596	1.572
r(C−H), Å		1.106 ± 0.005	1.094	1.075	1.088		1.087	1.106	
$\angle C_b-C_n-C_b$, (deg)		63.1 ± 0.2	62.69		63.5				
			62.66						
			62.67						
			62.67 ± 0.01[b]						
$\angle C_n-C_b-C_b$, (deg)		95.1 ± 0.1	95.81						
			95.78						
			95.57						
			94.99						
			95.15						
			95.46 ± 0.33[b]						
E (hartree)			−193.967	−192.691		−193.350	−193.511	−193.375	−193.370
Mulliken charge									
C_b			−0.016						
C_n			−0.538						
H			+0.274						
Lowdin charge									
C_b			−0.093						
C_n			−0.265						
H			+0.163						
C_b-C_b bond order									
Mulliken			−0.11						
Mayer			0.55						
n (ED)			0.70	0.73					

[a] C_b = bridgehead (axial) carbon atoms; C_n = methylene (equatorial) carbon atoms; ED = from electron density at the bond critical point. [b] Mean value.

atoms in terms of the hybridization of the atom-centered basis functions of the TZ94.bspp model, which are loosely related to the carbon 2s and 2p orbitals. The $3a_1'$ HOMO has very strong s character, due to strong s contributions from the bridgehead and methylene carbons. The bridgehead s contributions are in-phase (bonding). There is also a strong out-of-phase (bonding) bridgehead p contribution. The degenerate 1e″ orbitals have p character. There is essentially no s contribution to the bridgehead, and the p contribution is bonding. The 3e′ orbital has antibonding s and p contributions to the bridgehead, both of which are responsible for the p-like character of the 3e′ momentum profile. The $1a_2'$ orbital has essentially no contribution from the bridgehead carbons.

The studies of hybridization in [*l.m.n*]propellanes performed by several workers give contradictory results for [1.1.1]-propellane, the most-strained example.[17,46,19] The most recent study by Jarret and Cusumano[19] estimated the hybridization at the bridgehead carbons using $^{13}C-^{13}C$ NMR coupling constants. In contrast to the previous studies,[17,46] they found much higher p character ($sp^{8.6}-sp^{4.8}$) in the three hybrids forming the three bridgehead methylene bonds and much larger s character ($sp^{0.5}$) for the hybrids forming the interbridgehead bond. Since the HOMO makes a substantial contribution to the interbridgehead bond, a point in agreement with the very recent results of Kar and Jug,[47] and as we have previously seen that the HOMO is very s-like in nature (see Figure 2), the present results are not inconsistent with the observation of Jarret and Cusumano[19] in respect to the hybrid nature of the interbridgehead bond.

6. Conclusions

Using EMS techniques we have been able to *a priori* assess, for the extensive range of basis states investigated, the quality of these basis states and therefore the validity of the physical representation provided by our respective [1.1.1]propellane wave functions. This procedure enabled us to select our optimum wave function for [1.1.1]propellane, in this case a wave function calculated within a density functional theory framework at the triple-ζ level with Becke, Stoll, Pavlidou, and Preuss nonlocal functionals, from which the subsequently determined molecular properties were found to be in good accord with the available experimental data and other calculations. In particular, we confirmed the existence of the C1−C3 bridging bond with a bond order of $n = 0.70$.

Acknowledgment. One of us (M.J.B.) thanks the Australian Research Council (ARC) for the provision of a small grant and a QE2 Fellowship. W.v.N. acknowledges the Fonds der Chemischen Industrie for partial support while M.T.M. thanks CSIRO for travel support. The financial support of the Electronic Structure of Materials (ESM) Centre is also gratefully acknowledged by us all, as is Liz Milford for typing this manuscript. We thank Bob Nesbet for many stimulating discussions in relation to DFT.

JA963058F

(46) Herr, M. L. *Tetrahedron* **1977**, *33*, 1897.
(47) Kar, T.; Jug, K. *Chem. Phys. Lett.* **1996**, *256*, 201.